Effect of Alteration on the Geochemistry and Mechanical Properties of Granite from Pingjiang, Hunan Province, China

Minghao Ren (renmh@ncwu.edu.cn)
North China University of Water Resources and Electric Power https://orcid.org/0000-0003-1170-9931
Wei Wang
North China University of Water Resources and Electric Power
Zhiquan Huang
Luoyang Institute of Science and Technology
Shanggao Li
Zhongnan Engineering Corporation Limited
Qi Wu
North China University of Water Resources and Electric Power
Huaichang Yu
North China University of Water Resources and Electric Power
Guangxiang Yuan
North China University of Water Resources and Electric Power
Paul Sargent
Teesside University

Research Article

Keywords: Weathering, Hydrothermal alteration, Geochemistry, Mechanical properties, Granite

Posted Date: April 28th, 2021

DOI: https://doi.org/10.21203/rs.3.rs-467803/v1

Version of Record: A version of this preprint was published at Environmental Earth Sciences on January 20th, 2022. See the published version at https://doi.org/10.1007/s12665-022-10197-z.

Abstract

The effect of alteration on the geochemistry and mechanical properties of granite from Pingjiang, Hunan Province, China was investigated. Six weathered and 14 hydrothermally altered samples in three footrills (PD2, PD3, and PD4) were collected for mechanical tests and major and trace element analysis. The results show that the relationship between mechanical strength and the degree of alteration, irrespective of whether this is due to weathering or hydrothermal alteration, can be described by an exponential equation. This implies that the mechanical strength decreases rapidly even at low degrees of alteration. Granite Na_2O, CaO, K_2O, and SiO_2 contents were lowered due to weathering, whereas $Fe_2O_3{}^T$ contents increased significantly due to Fe^{2+} oxidation. Based on the hypothesis that Al and Zr are immobile during the hydrothermal alteration, the mobility indexes of various elements were calculated for the hydrothermally altered samples. In general, TiO_2, K_2O, $Fe_2O_3{}^T$, Th, Hf, Co, Ni, and V contents were unaffected by hydrothermal alteration; Na_2O, Sr, Nd, Sm, and Pb contents were lowered by hydrothermal alteration; and SiO_2, Rb, Cr, U, Zn, Mn, and Cs contents were increased due to reactions with the hydrothermal fluids. Even immobile elements, such as Sm, Nd, V, and Cr, were mobilized by high-temperature hydrothermal fluids. To assess the degree of hydrothermal alteration, a new model is required that can account for the effects of the different mineral components.

1. Introduction

The mineralogical, geochemical, and mechanical properties of rocks can be significantly changed by alteration (del Potro and Hürlimann, 2009; Huang et al., 2011; Julia et al., 2014; Moon and Jayawardane, 2004; Pola et al., 2012, 2014; Wang et al., 2015; Wyering et al., 2014). Almost all alteration occurs in two ways: (1) rocks interact with water and the atmosphere, which is called weathering (Fritz and Mohr, 1984; Moon and Jayawardane, 2004; Wang et al., 2013); and (2) hydrothermal fluids in contact with rocks cause water–rock reactions. The latter process is called hydrothermal alteration (Browne, 1978; Wyering et al., 2014).

The influence of weathering on the mechanical properties of rocks has been well studied (Arikan et al., 2007; Ceryan et al., 2008; Julia et al., 2014; Pola et al., 2012, 2014, Wyering et al., 2014). From previous studies, weathering process generally caused a reduction in strength and the mechanical properties of rocks show an obviously negative correlation with weathering grades (Arikan et al., 2007; Pola et al., 2012, 2014). According to Julia et al. (2014) and Wyering et al. (2014), The relationships between some parameters of rock strength (e.g., uniaxial compressive strength, compressional wave velocity, Young's modulus) and weathering grades could be described by exponential equations. The mineralogy transitions and chemical changes were also recognized during weathering and the clay minerals reduced the strength of rocks significantly (Arikan et al., 2007; Coggan et al., 2013; Wyering et al., 2014). While, few studies have focused on the geochemical changes during alteration, especially the hydrothermal alteration (Chigira et al., 2002; Duzgoren-Aydin et al., 2002; Sumner and Nel, 2002; Moon and Jayawardane, 2004; Yıldız et al., 2010; Wang et al., 2015). Typically, hydrothermal alteration occurs at higher temperatures and pressures as compared with weathering (Browne, 1978; Fritz and Mohr, 1984). Therefore, the effects of weathering and hydrothermal alteration on rocks should be significantly different. Moreover, the effects of alteration on the granite remain unclear. Given the sound mechanical properties of granite, hydroelectric dams are often situated on such rocks, including the Three Gorges Dam in China (Chen, 1999). The strength of the altered granite is directly related to the stability of the dam. However, the most published data are for weathered volcanic rocks, whereas weathered or hydrothermally altered granites have received little attention (Lan et al., 2003).

Here a case study on altered granite from Hunan Province, China, where a pumped storage hydroelectric station has been designed for construction on the granite, was reported. Six weathered and 14 hydrothermally altered samples were collected in three footrills (PD2, PD3, and PD4). Mechanical tests and major and trace element analyses of the granites were undertaken to: (1) investigate the effects of alteration on the mechanical properties of the granite; and (2) identify the geochemical changes during weathering and hydrothermal alteration, and examine the differences between these two processes.

2. Geological Background

The study area is located in the southern Yangtze Block where the regional structure is controlled by the deep Xinning–Miluo and Changsha–Pingjiang faults (Fig. 1). From north to south, this area is divided into four regions by these two faults: the Dongting rift basin, the Mufu Mountain–Ziyun Mountain uplift, the Pingjiang–Changsha rift basin, and the Lianyun Mountain–Hengyang Uplift (Fig. 1). The basement strata comprise the Lengjiaxi Group (Mesoproterozoic) and Banxi Group (Neoproterozoic). Due to tectonism, granite was widely intruded in this area from the Mesoproterozoic to Mesozoic, and particularly in the late Mesozoic.

A pumped storage hydroelectric station has been designed to be located in Fushou Mountain, which is in the northern part of the Pingjiang–Changsha rift basin (Fig. 2). The dams of both the upper and lower reservoirs would be constructed on a late Mesozoic granite intrusion. This granite was intruded into the Lengjiaxi Group at ca. 165 Ma (Xu et al., 2009; Zhang, 1991). Field investigations have shown that the structure of this area is controlled mainly by seven faults (Fig. 2) and joints developed in the intrusion. Quartz veins and pegmatite dikes are distributed around the faults.

The main rock type of this granite intrusion is monzogranite, which consists of quartz (20–52%), orthoclase (20–45%), plagioclase (20–35%), and biotite (2–8%). Albite is present in the orthoclase (Fig. 3a). A cataclastic texture was recognized in some samples (Fig. 3b). Due to weathering and hydrothermal alteration, biotite and feldspar are partly altered to chlorite (3–11%) and clay minerals (kaolinite, smectite, and illite; 3–25%), respectively (Fig. 3a–b). At the end of one footrill (PD2), a fault fracture zone is present (Fig. 2), where the granite has been brecciated and quartz veins have formed (Fig. 3c). During this process, the minerals in the granite were replaced by quartz, which resulted in silicification (Fig. 3d). The weathered samples were collected at the entrance of the footrill, showing the strong to completely weathered.

3. Analytical Methods

3.1 Mechanical tests

Velocities of ultrasonic P-waves (V_p) were calculated as follows: velocity = emission – receiver length/travel time. The size-corrected point load strength index ($I_{s(50)}$) was determined on irregular sample specimens, based on previously published methodologies (Kahraman et al., 2005; Moon and Jayawardane, 2004). The rock strength test was carried out *in situ* using the rebound method with a hammer. The rock strength is represented by the rebound value (R). This method was described in detail by Ma (2014).

3.2 Whole-rock major and trace elements

Whole-rock major and trace element abundances were analyzed at the State Key Laboratory of Geochemistry in the Guangzhou Institute of Geochemistry, Chinese Academy of Sciences, Guangzhou, China. A Rigaku ZSX100e X-ray fluorescence (XRF) spectrometer was used for major element determination, following the analytical procedures of Li et al. (2006). The analytical precision is generally better than ± 2%. Trace elements were determined with a Thermo X Series II inductively coupled plasma–mass spectrometer (ICP–MS) following the procedures of Li et al. (2006). The analytical precision was generally better than ± 5%.

4. Results

4.1 Mechanical tests

The mechanical test data are listed in Table 1. V_p for all samples varies from 0.35 to 6.11 km/s. Weathered samples yielded low V_p (< 1 km/s) due to high degree of weathering. The altered samples typically have relatively constant V_p (4–5 km/s). However, low V_p values (1.10–2.27 km/s) were obtained for some altered samples (Table 1). The point load strength index shows a large variation (4.71–76,273 kPa). Weathered samples have a low point load strength index (< 5 kPa). The rebound values of all samples range from 11 to 69. Weathered samples have low rebound values (11–24).

Table 1
Results of geochemical analysis and mechanical tests for granite samples in Pingjiang

Sample	PD 2 – 1	PD 2–2	PD 2–4	PD 2–5	PD 2–6	PD 2–7	PD 2–8	SPD 2–5	PD 2–9	PD 2–10	PD 2–11	SPD 2–4	SPD 2–3	XP 4-200	SPD 3 – 2	SPD 3–3
	Silicification zone					Fresh	Hydrothermal altered								Weathered	
Major oxides (%)																
Na_2O	3.74	3.84	1.87	3.53	3.15	3.70	3.97	3.50	3.89	4.11	4.14	3.41	3.17	2.76	2.46	3.81
MgO	0.31	0.47	0.23	0.47	0.45	0.65	0.56	0.68	0.53	0.50	0.48	0.71	0.65	0.40	0.80	0.91
Al_2O_3	12.0	12.3	7.20	12.1	12.7	15.4	15.0	14.9	15.5	15.2	16.1	14.9	15.3	14.8	17.6	14.8
SiO_2	77.4	75.9	85.6	76.7	76.3	70.7	72.0	72.1	71.1	71.2	70.7	71.8	71.8	72.7	68.4	71.0
K_2O	2.80	3.24	1.57	2.87	2.97	3.58	3.43	3.31	4.11	4.15	2.83	3.29	3.20	4.95	2.96	2.39
CaO	1.41	1.01	1.34	1.00	1.40	2.59	1.50	2.64	0.72	0.38	2.55	2.64	2.50	1.47	1.80	2.97
TiO_2	0.18	0.23	0.11	0.23	0.22	0.27	0.24	0.21	0.27	0.25	0.23	0.23	0.22	0.12	0.27	0.28
$Fe_2O_3{}^T$	1.27	1.72	0.88	1.73	1.49	1.92	1.63	1.74	1.87	1.83	1.68	2.01	1.82	1.26	2.43	2.51
LOI	0.69	0.85	0.53	1.18	1.09	0.74	1.02	0.97	1.41	1.58	0.84	1.01	1.35	1.52	3.29	1.35
Trace elements (ppm)																
V	21.6	26.6	26.4	18.3	21.9	26.4	21.2	-	21.2	19.2	17.2	-	-	-	-	-
Cr	5.18	14.0	7.99	6.49	6.50	7.99	7.04	7.74	5.68	6.43	5.75	8.60	8.10	5.88	9.34	9.13
Mn	176	565	219	246	265	219	212	220	203	236	215	262	240	337	337	414
Co	2.17	3.19	3.32	2.91	2.39	3.32	2.94	-	2.59	2.48	2.33	-	-	-	-	-
Ni	1.96	2.39	3.11	2.30	2.34	3.11	2.69	3.63	2.66	2.01	2.40	4.16	4.21	2.29	4.02	4.52
Zn	48.6	52.2	56.7	61.2	64.0	56.7	69.8	55.7	50.5	69.5	51.0	74.9	62.6	191	77.9	80.3
Rb	133	5.99	172	178	213	172	172	-	181	202	130	-	-	-	-	-
Sr	314	71.5	605	303	451	605	603	-	301	194	459	-	-	-	-	-
Zr	92.4	124	156	138	128	156	148	-	128	121	117	-	-	-	-	-
Cs	7.08	0.33	8.67	13.5	17.1	8.67	7.93	-	10.2	9.93	27.6	-	-	-	-	-
Ba	740	77.1	1062	950	947	1062	1108	-	836	890	816	-	-	-	-	-
Nd	11.5	19.4	27.6	9.00	15.9	27.6	26.6	-	20.8	23.4	17.6	-	-	-	-	-
Sm	1.79	4.41	4.18	1.47	2.43	4.18	4.00	-	3.35	3.48	2.71	-	-	-	-	-
Hf	2.75	3.44	4.48	3.93	3.55	4.48	4.17	-	3.96	3.71	3.67	-	-	-	-	-
Pb	14.1	6.29	43.2	33.8	36.1	43.2	46.0	42.9	43.7	38.2	40.5	50.7	60.9	553	43.0	44.2
Th	9.57	3.93	14.7	14.3	12.5	14.7	15.0	-	13.6	13.0	12.3	-	-	-	-	-
U	2.91	1.29	2.85	4.65	3.05	2.85	2.69	-	2.25	2.92	1.54	-	-	-	-	-
Mechanical tests																
V_p (Km/s)	2.00	1.10	4.04	4.88	5.11	4.33	4.23	4.21	4.50	3.92	4.86	3.69	1.49	6.11	0.51	0.55
$I_{s(50)}$ (Kpa)	4468	5382	5053	4069	1036	4991	4310	5946	2930	364	2948	838	50.0	76273	4.69	5.04
Rebound value	28	32	28	29	25	30	32	56	30	25	31	24	22	69	11	20

4.2 Whole-rock major and trace elements

The major and trace element data are listed in Table 1. Compared with altered samples, the weathered samples have higher concentrations of MgO (0.60–2.55 wt.%) and $Fe_2O_3{}^T$ (2.13–9.90 wt.%), and lower contents of Na_2O (0.32–3.81 wt.%), K_2O (1.57–3.22 wt.%), and CaO (0.67–2.97 wt.%). Due to silicification,

one sample (PD2-4) has a very high SiO_2 content (85.59 wt.%). The loss-on-ignition (LOI) values vary from 2.35 to 8.14 and 0.53 to 1.58 wt.% for weathered and altered samples, respectively. In general, the trace element contents of weathered samples are higher than those of altered samples (Table 1).

5. Discussion

5.1 Effects of alteration on the mechanical properties of granite

Previous studies have shown that hydrothermal alteration effects on rocks depend on a number of factors, including fluid type and $P–T$ conditions (Frolova et al., 2012; Julia et al., 2014). Under most conditions, weathering significantly reduces the mechanical strength of rocks (Julia et al., 2014; Moon and Jayawardane, 2004). However, alteration is not always related to a reduction in mechanical strength (Pola et al., 2014; Watters, 2000).

Some altered samples in PD2 have similar or even higher values of mechanical strength as compared with fresh samples (Fig. 4). These samples were all distributed in the silicified fracture zone. During this process, Si-rich hydrothermal fluids reacted with country rocks and primary minerals were replaced by quartz. Thus, silicification can strengthen a granite. For the other altered samples, chloritization and argillization were the dominant alteration types. The samples in PD2 have relatively low values for mechanical parameters, especially for V_p and $I_{s(50)}$ (Fig. 4). This demonstrates that argillization and chloritization weaken the granite.

The LOI value is assumed to represent the water retained within a rock and its minerals, which is regulated by the degree of weathering (Moon and Jayawardane, 2004; Pola et al., 2012). Hydrothermal alteration is caused by the movement of hot, dissolved-ion-rich fluids through reservoir rocks causing dissolution, mineral deposition, and clay mineral formation (Hurwitz et al., 2002; Pola et al., 2012, 2014; Wyering et al., 2014). Water can be incorporated into the structures of secondary minerals (Julia et al., 2014). Therefore, the LOI value is also an indicator of the degree of hydrothermal alteration. From the The relationships between the three mechanical parameters and LOI values could be roughly described by exponential equations (Fig. 5a–c). The mechanical parameters of the hydrothermally altered samples decline rapidly. This is similar to the conclusions reported by Julia et al. (2014) and Wyering et al. (2014). The exponential relationship between mechanical strength and degree of alteration implies that mechanical strength decreases rapidly at low degrees of alteration. For samples from PD2, $I_{s(50)}$ decreases by two orders of magnitude from LOI = 1 to 2 wt.% (Fig. 5d).

In addition, the mechanical strength of the weathered and hydrothermal altered samples varied with LOI as a same relationship, indicating that the two altered processes weakened the granite with a common reason. From the previous studies (Julia et al., 2014; Wyering et al., 2014) and thin-section observation, the alteration of minerals during the weathered and hydrothermal altered samples are similar. In this study, the biotite and feldspar in the weathered and hydrothermal altered granite are wholly to partly converted to chlorite and clay minerals, respectively (Fig. 3a–b). Therefore, the reduction of the rock strength during the two altered processes may be attributed to the mineral alteration.

5.2 Geochemical changes due to alteration

In general, mineral alteration are accompanied by geochemical variations. Many studies have documented geochemical changes resulting from weathering of rocks (Aiuppa et al., 2000; Chigira et al., 2002; Duzgoren-Aydin et al., 2002; Fritz and Mohr, 1984; Guan, 2001; Lan et al., 2003; Moon and Jayawardane, 2004; Sharma and Rajamani, 2000), but few studies have considered the effects of hydrothermal alteration (Wang et al., 2013; Wyering et al., 2014). From these previous studies, it is apparent that Na, Ca, Si, K, and Mg are mobile, whereas Zr, Ti, and Al are immobile during weathering. Thus, Na_2O, CaO, SiO_2, K_2O, and MgO would be leached from rocks during weathering. FeO would be oxidized to Fe_2O_3 during weathering, thereby increasing the total Fe_2O_3 content ($Fe_2O_3{}^T$) (Aiuppa et al., 2000; Chigira et al., 2002; Guan, 2001; Moon and Jayawardane, 2004). Most trace element concentrations increase in the early weathering stages, but decrease with further weathering. This increase during the early stages is likely a reflection of the loss of major elements, while the reduction likely represents the mobilization of trace elements during argillization (Aiuppa et al., 2000; Moon and Jayawardane, 2004). Rubidium and Sr behave similarly to Ca during weathering because of their similar ionic radii (Moon and Jayawardane, 2004).

The results for weathered samples are similar to those of previous studies. Na_2O, CaO, K_2O, and SiO_2 contents in the weathered samples show negative correlations with LOI values (Fig. 6a–d), which means the contents of these elements decreased during weathering. Due to the oxidation of Fe^{2+} in the weathered samples, $Fe_2O_3{}^T$ concentrations increase significantly (Fig. 6f). However, MgO behaves differently than described in some previous studies (Guan, 2001; Moon and Jayawardane, 2004). MgO contents in the weathered samples show a positive correlation with LOI values, indicating the samples gained MgO during weathering (Fig. 6e). A similar increase in MgO contents in weathered samples was reported by Chigira et al. (2002). Previous studies of element mobility during weathering have assumed the same mineral compositions in all rock samples (Aiuppa et al., 2000; Chigira et al., 2002; Guan, 2001; Moon and Jayawardane, 2004). In fact, rock samples are heterogeneous and mineral compositions are variable, even in samples from the same location. Thus, the inconsistent behavior of MgO may be attributed to variations in mineral compositions.

As compared with weathered samples, major and trace element contents of hydrothermally altered samples show no clear relationships with LOI values (Fig. 6). Chloritization, argillization, and silicification were the dominant hydrothermal alteration types. Based on fieldwork and petrological observations, the samples from PD2 have similar mineral compositions. Therefore, these samples are ideal for assessing element mobility due to weathering. The method described by Guan et al. (2001) was used to compute the mobility index (MI) of elements due to hydrothermal alteration. The calculated activities of Al species in many hydrothermal systems are very low, and Al is conserved during the conversion of biotite to chlorite (Helgeson, 1970; Parry and Downey, 1982). Zirconium is an immobile element and is immobile during alteration. In this study, Al_2O_3 and Zr were taken to be immobile elements and the unaltered sample PD2-7 was used as the baseline sample to assess alteration effects. The MI of each element was then calculated as follows:

$$MI = (R^i_a/R_a)/(R^i_p/R_p) \quad (1)$$

where R^i_a is the weight percentage of mobile element *i* in the altered sample, R_a is the weight percentage of immobile elements in the altered sample, R^i_p is the weight percentage of mobile element *i* in the unaltered sample, and R_p is the weight percentage of immobile elements in the unaltered sample.

The calculated MIs for major elements normalized to Al_2O_3 are shown in Fig. 7. The MIs of TiO_2 (average MI = 0.93 ± 0.10), K_2O (average MI = 1.00 ± 0.12), and $Fe_2O_3{}^T$ (average MI = 0.97 ± 0.10) are near unity (i.e., immobile), whereas MIs for Na_2O, MgO, CaO, and SiO_2 are variable, especially for samples from the area of silicification (Fig. 7). In general, CaO and MgO were leached out during alteration. Na_2O and SiO_2 were enriched in the samples that underwent silicification, but remained relatively constant in the other samples. MIs of trace elements have a wider range as compared with major elements (Fig. 7). Average MIs for Th, Hf, and some transition metals (e.g., Co, Ni, and V) are near unity (i.e., immobile). In general, Sr, Nd, Sm, and Pb have MI < 1, whereas Rb, Cr, U, Zn, Mn, and Cs have MI > 1. However, the samples show different characteristics depending on the nature of alteration (i.e., chloritization, argillization, or silicification).

5.3 Differences in element mobilities due to hydrothermal alteration

Argillization, chloritization, and silicification occur under different thermal conditions and by distinct processes. Argillic rocks are formed at low temperatures (50–150°C) (Julia et al., 2014). During the early stages of argillization, plagioclase reacts with K-rich acidic hydrothermal fluids, forming smectite/illite. As the reaction proceeds, H^+ replaces K^+ in K-feldspar and smectite/illite, forming kaolinite. The major compositional change in the rock is the removal of Ca and Na, and some Mg. Potassium tends to remain constant, or slightly increases and then decreases (Hemley and Jones, 1964). Thus, changes in K and the loss of Ca and Mg in the altered samples of this study are attributed mainly to argillization (Fig. 7). The behavior of alkali elements similar to Ca and K (e.g., Rb, Sr, Ba, and Cs) can also be attributed to this process. However, changes in Na are not consistent with argillization, as almost all the samples gained Na (Fig. 7). Thin-section observations revealed that orthoclase was partly altered to albite (Fig. 3a). During this process, K in orthoclase is replaced by Na, thereby increasing the Na concentration. Therefore, the formation of albite might be responsible for the increases in Na in the altered samples.

The temperatures of chlorite formation are 150–300°C (Huang, 2017). Previous studies have concluded that the alteration of biotite to chlorite in granite conserves Al and results in K and Ti loss and Mg and Mn gain (Parry and Downey, 1982). Therefore, the high MI for Mg (MIs for Mg in three samples are > 1) and Mn can be attributed to chloritization. Given the affinity between Mn, Zn, and Cr, this can also explain the gain of Zn and Cr in these samples.

Silicification occurs due to reactions with high-temperature fluids (T = 300–550°C) (Julia et al., 2014). This process significantly increases SiO_2 concentrations of samples in two ways: SiO_2 derived from the hydrothermal fluids and by decomposition of feldspar to clay minerals (e.g., argillization; Lv et al., 2011). In this study, the MIs of SiO_2 in the non-silicified samples are all near unity (Fig. 7). As such, silicification associated with argillization was negligible. Therefore, the SiO_2 added to the silicified samples was derived from hydrothermal fluids. The mobilities of Sm, Nd, V, and Cr in silicified samples differ from those of the non-silicified samples. The MIs of Sm, Nd, V, and Cr in the non-silicified samples are near unity, indicating limited mobility during argillization and chloritization (Fig. 7). These four elements tend to be immobile during weathering (Aiuppa et al., 2000; Fritz and Mohr, 1984; Sharma and Rajamani, 2000). However, MIs of these elements in the silicified samples have a wide range of values. As such, these elements were more mobile during silicification, possibly due to the high fluid temperatures.

One silicified sample (PD2-2) has a distinct trace element pattern (Fig. 7). This sample lost large amounts of Sr, Pb, Ba, Th, Rb, and Cs (alkali elements) and gained large amounts of Mn and Zn. It also has the largest MI for Na (1.30) and lowest MI for Ca (0.49). This can be attributed to extensive albitization and chloritization.

6. Conclusions

We investigated the effects of alteration on the mechanical properties of granite using mechanical tests and geochemical data. Weathered granites have a very low mechanical strength. Granite is weakened by argillization and chloritization, whereas it is strengthened by silicification. The relationship between mechanical strength and degree of alteration (weathering and hydrothermal alteration) can be described by an exponential equation. As such, mechanical strength decreases rapidly at low degrees of alteration.

Granite Na_2O, CaO, K_2O, and SiO_2 contents decrease due to weathering. $Fe_2O_3{}^T$ concentrations increase significantly due to Fe^{2+} oxidation. Based on the stable constituent hypothesis, MIs of elements were calculated for hydrothermally altered samples to assess element behavior during hydrothermal alteration. In general, TiO_2, K_2O, $Fe_2O_3{}^T$, Th, Hf, Co, Ni, and V were immobile during hydrothermal alteration. Na_2O, Sr, Nd, Sm, and Pb were lost, whereas SiO_2, Rb, Cr, U, Zn, Mn, and Cs were added, during reactions with hydrothermal fluids. Silicification increased SiO_2 contents and mobilized some immobile elements, such as Sm, Nd, V, and Cr.

The evaluation of element mobility was based on the assumption of congruent weathering. This limits the application of this method. A new theoretical model that takes into account incongruent mineral weathering needs to be developed to quantitatively define the effects of hydrothermal alteration.

Declarations

Funding information:

This study is financially supported by grants from a National Key R&D Program of China (Grant No. 2019YFC1509704), the Natural Science Foundation of China (Grant No. 41803033, 41903034), Central Plains Science and Technology Innovation Leader Project (Grant No. 214200510030) and the Research Foundation of North China University of Water Resources and Electric Power (No. 20171003).

Acknowledgements

This study is financially supported by grants from a National Key R&D Program of China (Grant No. 2019YFC1509704), the Natural Science Foundation of China (Grant No. 41803033, 41903034), Central Plains Science and Technology Innovation Leader Project (Grant No. 214200510030) and the Research Foundation of North China University of Water Resources and Electric Power (No. 20171003). We thank Shengping Qian, Guangqian Hu, Yezhi He, Shengling Sun for their assistance in laboratory anaylsis. The authors have declared that no conflict of interest exists.

References

1. Aiuppa A, Allard P, D'Alessandro W, Michel A, Parello F, Treuil M, Valenza M (2000) Mobility and fluxes of major, minor and trace metals during basalt weathering and groundwater transport at Mt. Etna volcano (Sicily). Geochimica Et Cosmochimica Acta 64:1827–1841
2. Arıkan F, Ulusay R, Aydın N (2007) Characterization of weathered acidic volcanic rocks and a weathering classification based on a rating system. Bull Eng Geol Env 66:415–430
3. Browne PRL (1978) Hydrothermal Alteration in Active Geothermal Fields. Annu Rev Earth Planet Sci 6:229–250
4. Ceryan S, Tudes S, Ceryan N (2008) Influence of weathering on the engineering properties of Harsit granitic rocks (NE Turkey). Bull Eng Geol Env 67:97–104
5. Chen D (1999) Engineering geological problems in the Three Gorges Project on the Yangtze, China. Eng Geol 51:1–11
6. Chigira M, Nakamoto M, Nakata E (2002) Weathering mechanisms and their effects on the landsliding of ignimbrite subject to vapor-phase crystallization in the Shirakawa pyroclastic f low, northern Japan. Eng Geol 66:111–125
7. Del Potro R, Hürlimann M (2009) The decrease in the shear strength of volcanic materials with argillic hydrothermal alteration, insights from the summit region of Teide stratovolcano, Tenerife. Eng Geol 104:135–143
8. Duzgoren-Aydin NS, Aydin A, Malpas J (2002) Re-assessment of chemical weathering indices: case study on pyroclastic rocks of Hong Kong. Eng Geol 63:99–119
9. Fritz SJ, Mohr DW (1984) Chemical alteration in the micro weathering environment within a spheroidally-weathered anorthosite boulder. Geochimica Et Cosmochimica Acta 48:2527–2535
10. Frolova YV, Ladygin VM, Rychagov SN (2012) Patterns in the transformation of the composition and properties of volcanogenic rocks in hydrothermal-magmatic systems of the Kuril-Kamchatka island arc. Mosc Univ Geol Bull 66:430–438
11. Guan P, Ng CWW, Sun M, Tang W (2001) Weathering indices for rhyolitic tuff and granite in Hong Kong. Eng Geol 59:147–159
12. Helgeson HC (1970) Description and interpretation of phase relations in geochemical processes involving aqueous solutions. Am J Sci 268:415–438
13. Hemley JJ, Jones WR (1964) Chemical aspects of hydrothermal alteration with emphasis on hydrogen metasomatism. Econ Geol 59:538–569
14. Huang JH (2017) Alteration mineral geochemistry of VMS deposit- case study of the Honghai Cu-Zn deposit, Eastern Tianshan, NW China. Dissertation, University of Chinese Academy of Sciences. (in Chinese with English abstract)
15. Huang ZQ, Wang Z, Hou HM (2011) Alteration and engineering characteristics of altered-rock in Tianchi Pumped-storage power station. Journal of North China Institute of Water Consevancy Hydroelectric Power 32:1–5. (in Chinese with English abstract)
16. Hurwitz S, Ingebritsen SE, Sorey ML (2002) Episodic thermal perturbations associated with groundwater flow: An example from Kilauea Volcano, Hawaii. J Geophys Res 107:1301–1310
17. Julia F, Vladimir L, Sergey R, David Z (2014) Effects of hydrothermal alterations on physical and mechanical properties of rocks in the Kuril–Kamchatka island arc. Eng Geol 183:1–16
18. Kahraman S, Gunaydin O, Fener M (2005) The effect of porosity on the relation between uniaxial compressive strength and point load index. Int J Rock Mech Min Sci 42:584–589
19. Lan HX, Hu RL, Yue ZQ, Lee CF, Wang SJ (2003) Engineering and geological characteristics of granite weathering profiles in South China. journal of Asian Earth Sciences 21:353–364
20. Li XH, Li ZX, Wingate MTD, Chung SL, Liu Y, Lin GC, Li WX (2006) Geochemistry of the 755Ma Mundine Well dyke swarm, northwestern Australia: Part of a Neoproterozoic mantle superplume beneath Rodinia? Precambr Res 146:1–15
21. Lv CX, Wu GG, Chen XL, Zhang YC, Zhang XY, Zhao H (2011) Structural and geochemical characteristics of alteration zone of Xincheng gold deposit. Geotectonica et Metallogenia 35:618–627. (in Chinese with English abstract)
22. Ma TF (2014) Research on High strength concrete strength survey based on rebound method in Hebei. Dissertation, Hebei University of Technology. (in Chinese with English abstract)
23. Moon V, Jayawardane J (2004) Geomechanical and geochemical changes during early stages of weathering of Karamu Basalt, New Zealand. Eng Geol 74:57–72
24. Parry WT, Downey LM (1982) Geochemistry of hydrothermal chlorite replacing igneous biotite. Clays Clay Miner 30:81–90
25. Pola A, Crosta G, Fusi N, Barberini V, Norini G (2012) Influence of alteration on physical properties of volcanic rocks. Tectonophysics 566–567:67–86
26. Pola A, Crosta GB, Fusi N, Castellanza R (2014) General characterization of the mechanical behaviour of different volcanic rocks with respect to alteration. Eng Geol 169:1–13
27. Sharma A, Rajamani V (2000) Major Element, REE, and Other Trace Element Behavior in Amphibolite Weathering under Semiarid Conditions in Southern India. J Geol 108:487–496

28. Sumner P, Nel W (2002) The effect of rock moisture on Schmidt hammer rebound: tests on rock samples from Marion Island and South Africa. Earth Surf Process Landforms 27:1137–1142
29. Wang AM, Li XG, Huang ZQ, Huang XC, Wang ZF, Wu Q, Cui JL, Lu XJ (2015) Laboratory study on engineering geological characteristics and formation mechanism of altered rocks of Henan Tianchi pumped storage power station, China. Environ Earth Sci 74:5063–5075
30. Wang AM, Zhou J, Zhong FW, Wu Q, Cui JL (2013) Characteristics Analysis of Rock Weathering and Alteration for Tianchi Pumped Storage Power Station. Journal of North China Institute of Water Consevancy Hydroelectric Power 8:21–25. (in Chinese with English abstract)
31. Watters (2000) Rock Mass Strength Assessment and Significance to Edifice Stability, Mount Rainier and Mount Hood, Cascade Range Volcanoes. Pure applied geophysics 157:957–976
32. Wyering LD, Villeneuve MC, Wallis IC, Siratovich PA, Kennedy BM, Gravley DM, Cant JL (2014) Mechanical and physical properties of hydrothermally altered rocks, Taupo Volcanic Zone, New Zealand. J Volcanol Geoth Res 288:76–93
33. Xu DR, Wang L, Li PC, Chen GH, He ZL, Fu GG, Wu J (2009) Petrogenesis of Lianyunshan granites in northeastern Hunan Province, South China, and its geodynamic implications. Acta Petrologica Sinica 25:1–23. (in Chinese with English abstract)
34. Yıldız A, Kuşcu M, Dumlupunar I, Arıtan AE, Bağcı M (2010) The determination of the mineralogical alteration index and the investigation of the efficiency of the hydrothermal alteration on physico-mechanical properties in volcanic rocks from Köprülü, Afyonkarahisar, West Turkey. Bulletin of engineering geology the environment 69:51–61
35. Zhang W (1991) Structural and geochemical features of the Changsha-Pingjiang fracture dynamic metamorphism zone in NE. Hunan Province, China. Geotectonica et Metallogenia 100–109. (in Chinese with English abstract)

Figures

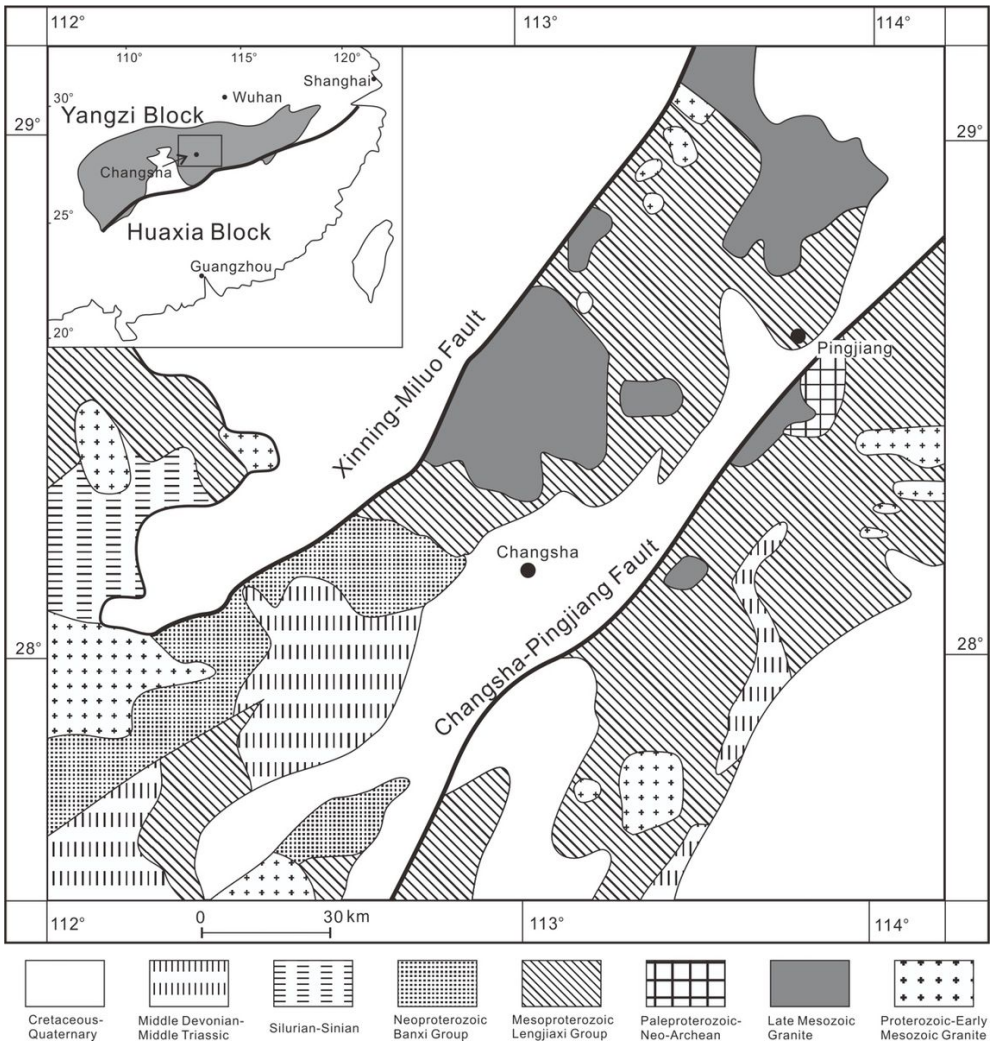

Figure 1

Geological map of Pingjiang (modified from Xu et al., 2009). Note: The designations employed and the presentation of the material on this map do not imply the expression of any opinion whatsoever on the part of Research Square concerning the legal status of any country, territory, city or area or of its authorities, or concerning the delimitation of its frontiers or boundaries. This map has been provided by the authors.

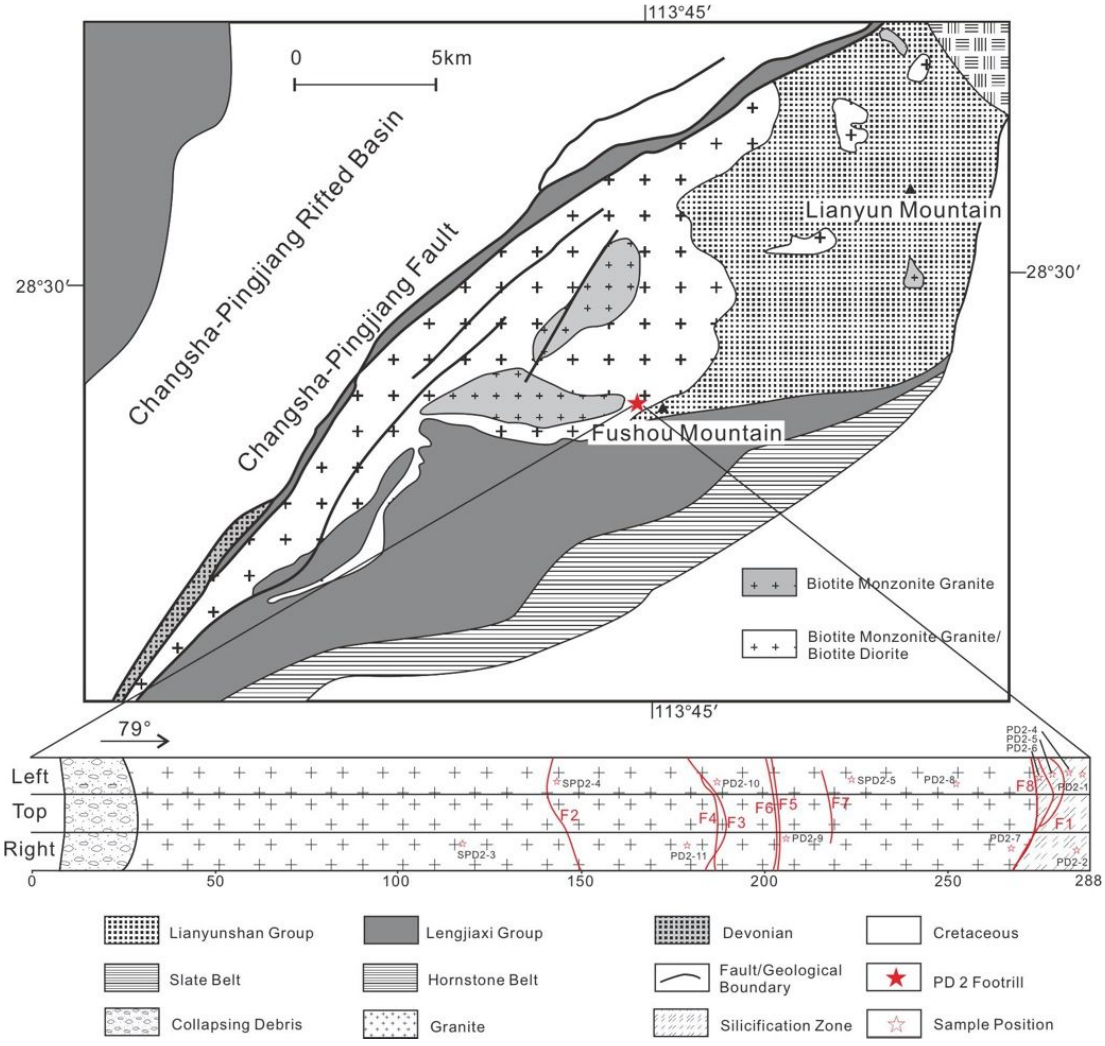

Figure 2

Geological map of Fushou mountain and geological sketch of the PD2 footrill (modified from Xu et al., 2009). Note: The designations employed and the presentation of the material on this map do not imply the expression of any opinion whatsoever on the part of Research Square concerning the legal status of any country, territory, city or area or of its authorities, or concerning the delimitation of its frontiers or boundaries. This map has been provided by the authors.

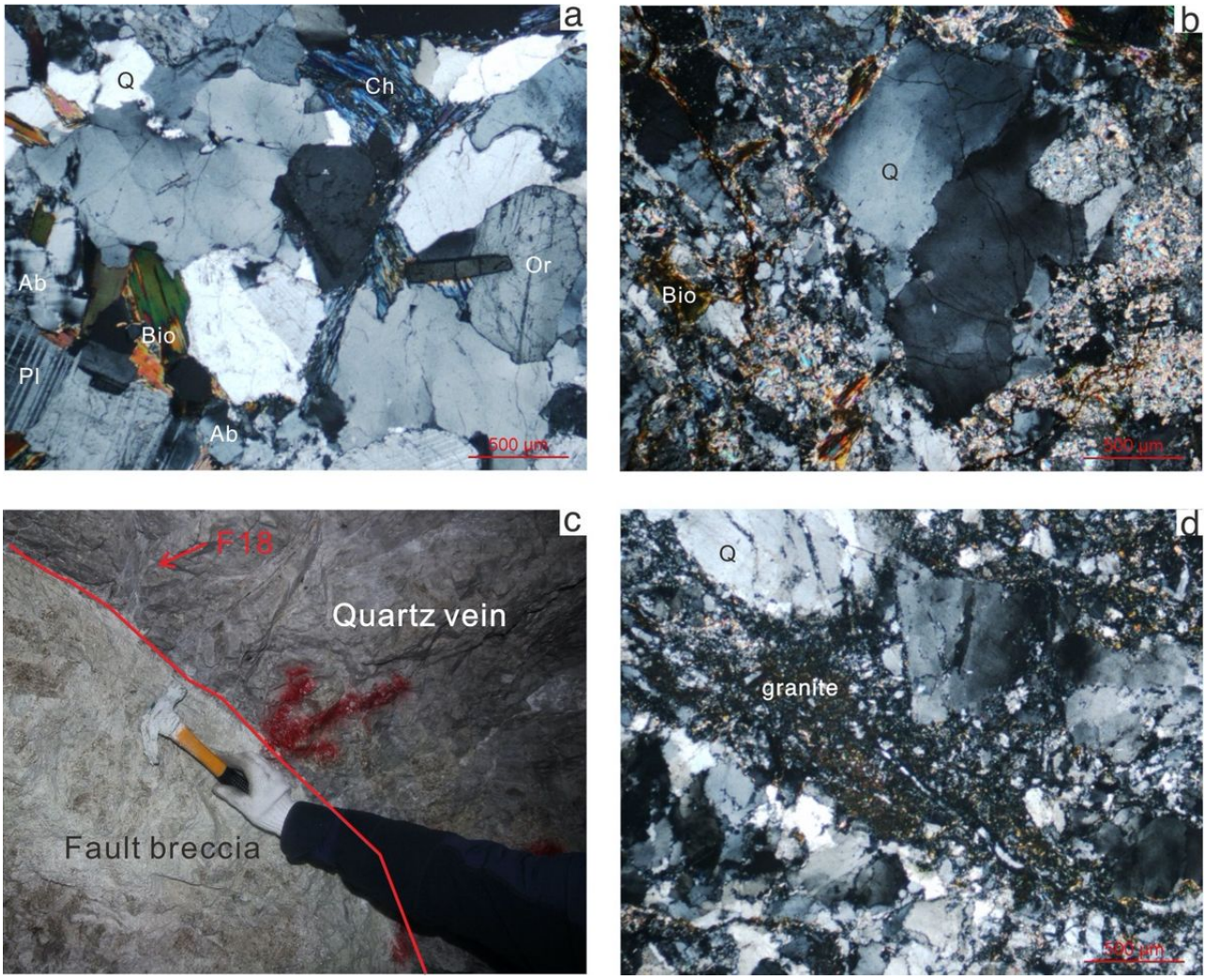

Figure 3

Photomicrographs of thin section and photographs of silicification zone. (a) Biotite and orthoclase were partly altered to chlorite and albite, respectively. (b) Cataclastic texture is well develop and feldspars were altered to argillic minerals. (c) Granite is broken into breccia and quartz refilled at the end of PD2. (d) Granite is replaced by quartz. Abbreviations: Ab=albite, Bio=biotite, Ch=chlorite, Or=orthoclase, Pl=plagioclase, Q=quartz. Note: The designations employed and the presentation of the material on this map do not imply the expression of any opinion whatsoever on the part of Research Square concerning the legal status of any country, territory, city or area or of its authorities, or concerning the delimitation of its frontiers or boundaries. This map has been provided by the authors.

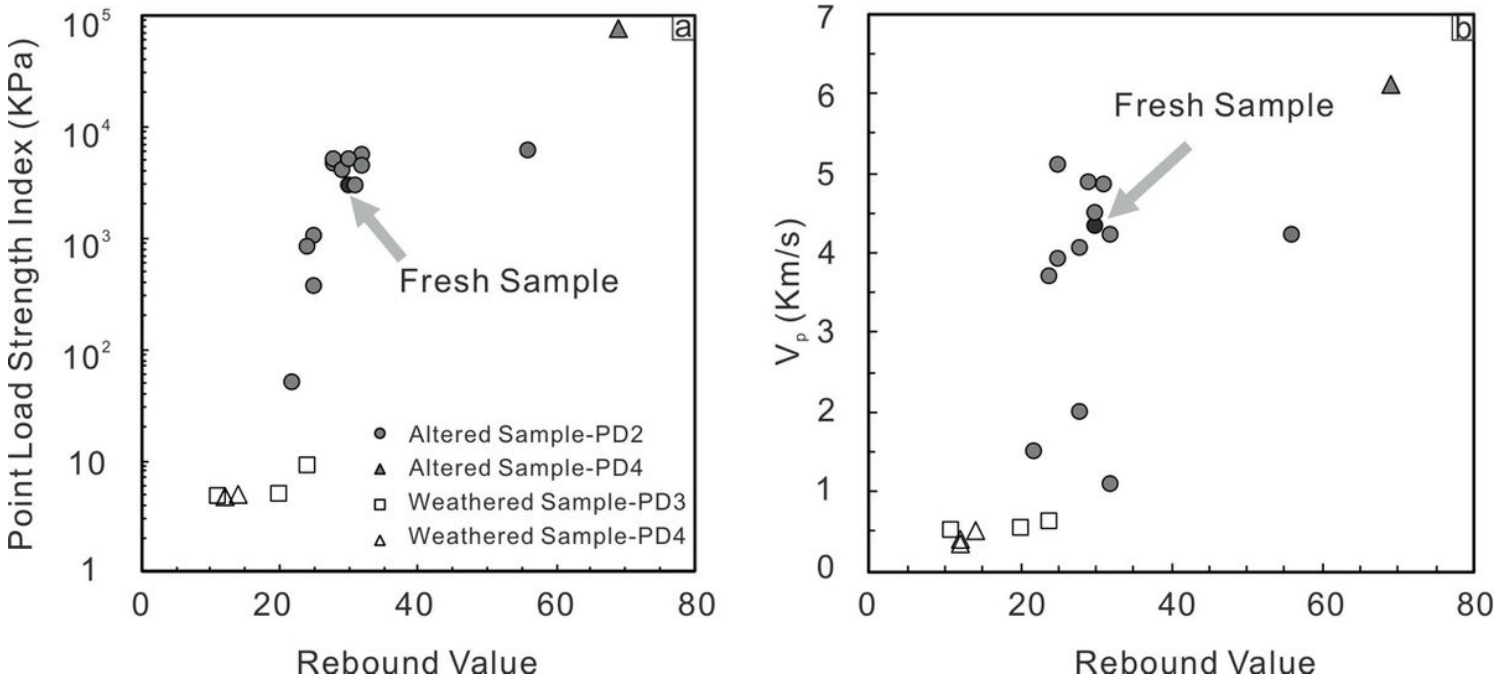

Figure 4

Plots of rebound value versus point load strength index (a) and Vp (b).

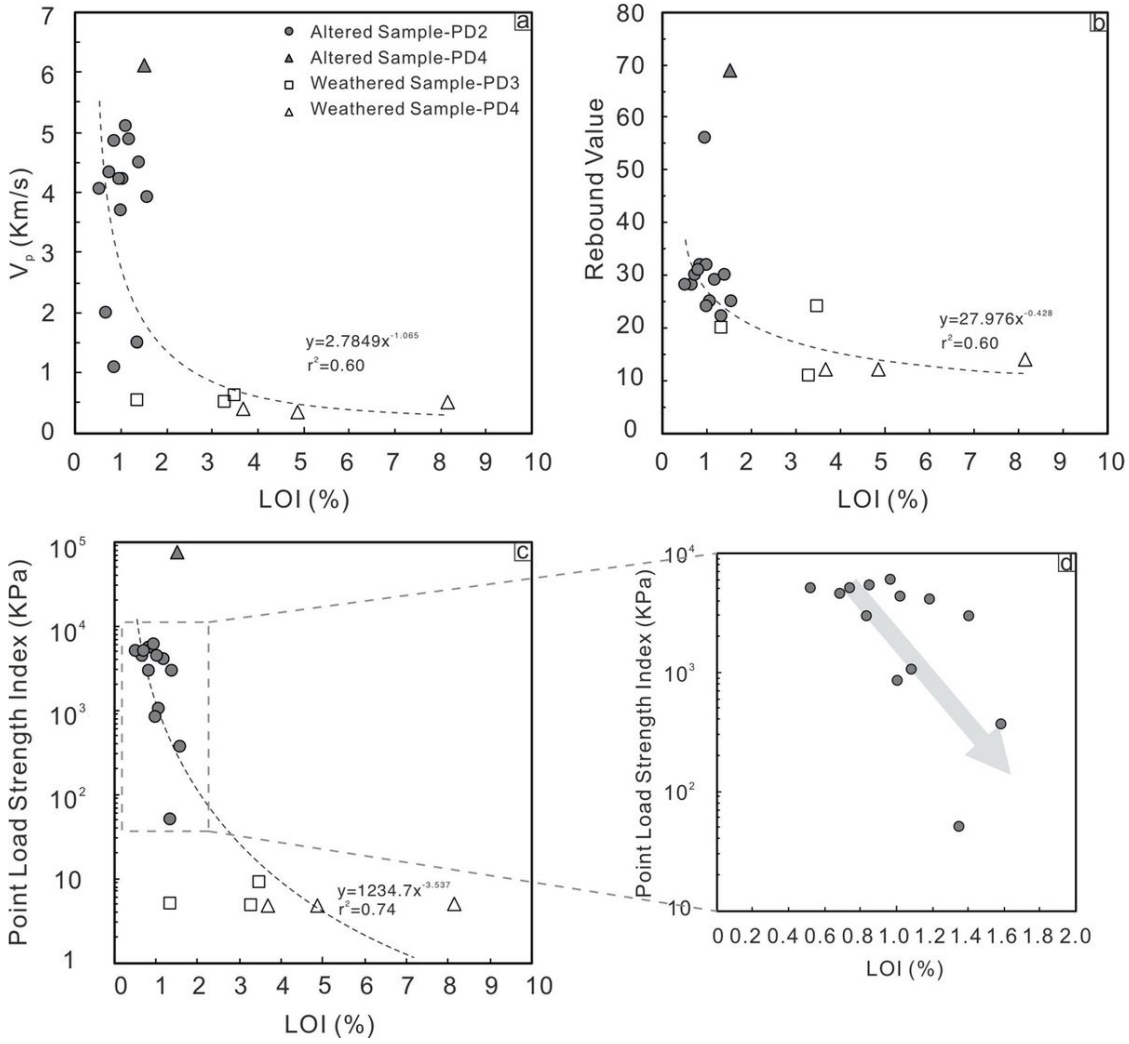

Figure 5

Plots of LOI versus Vp (a), rebound value (b) and point load strength index (c, d).

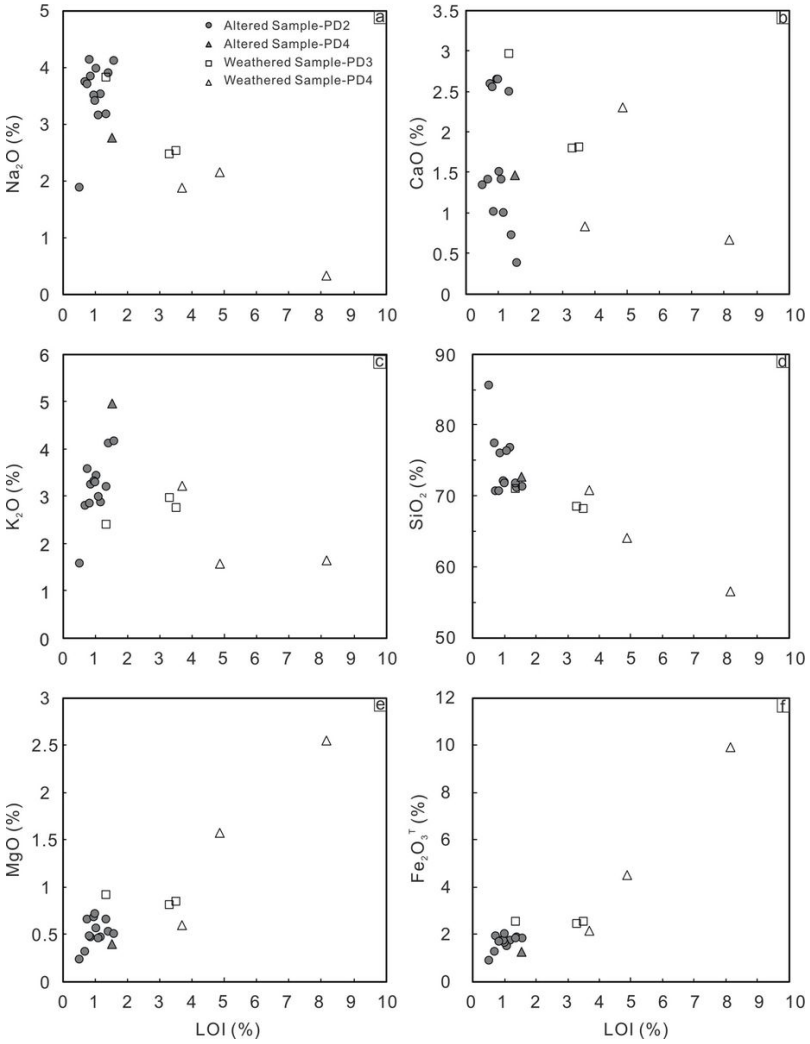

Figure 6

Plots of LOI versus Na2O (a), CaO (b), K2O (c), SiO2 (d), MgO (e) and Fe2O3T (f).

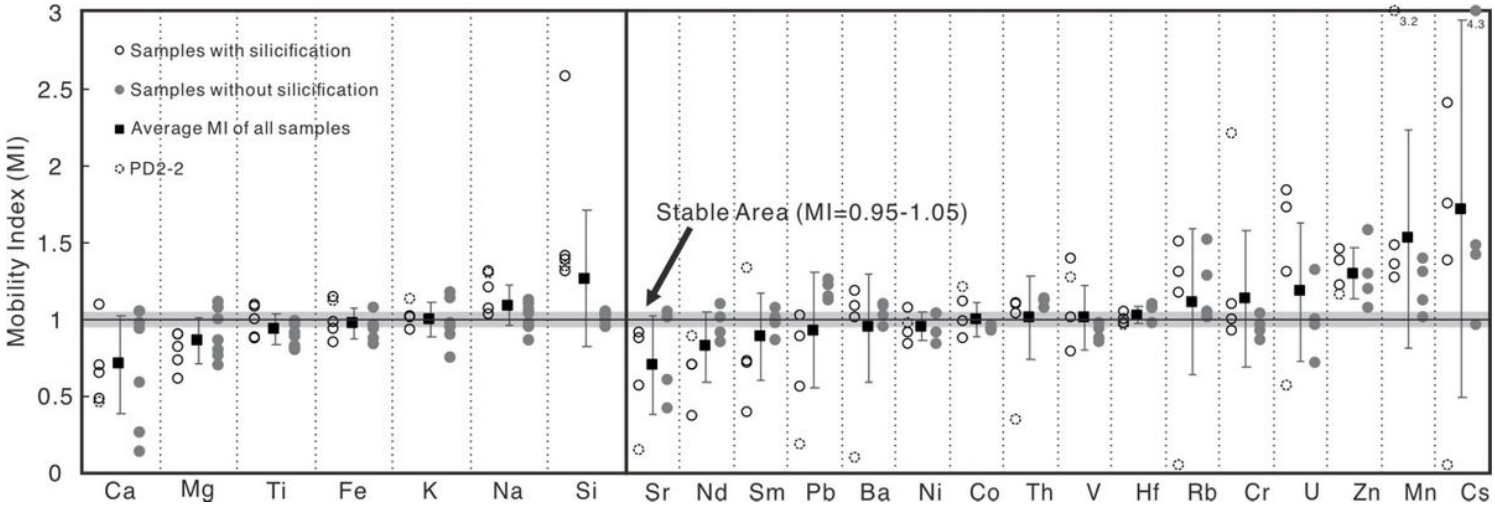

Figure 7

MIs of major elements and trace elements normalized to Al2O3 and Zr, respectively.